Applying a free-water correction to diffusion imaging data uncovers stress-related neural pathology in depression

Maurizio Bergamino[a,1], Ofer Pasternak[b,2], Madison Farmer[a,1], Martha E. Shenton[b,c,2], J. Paul Hamilton[a,d,*,3]

[a] Laureate Institute for Brain Research, Tulsa, OK, USA
[b] Department of Psychiatry and Radiology, Brigham and Women's Hospital, Harvard Medical School, Boston, MA, USA
[c] VA Boston Healthcare System, Boston, MA, USA
[d] Center for Social and Affective Neuroscience, Department of Clinical and Experimental Medicine, Linköping, Sweden

ABSTRACT

Diffusion tensor imaging (DTI) holds promise for developing our understanding of white-matter pathology in major depressive disorder (MDD). Variable findings in DTI-based investigations of MDD, however, have thwarted development of this literature. Effects of extra-cellular free-water on the sensitivity of DTI metrics could account for some of this inconsistency. Here we investigated whether applying a free-water correction algorithm to DTI data could improve the sensitivity to detect clinical effects using DTI metrics. Only after applying this correction, we found: a) significantly decreased fractional anisotropy and axial diffusivity (AD) in the left inferior fronto-occipital fasciculus (IFOF) in MDD; and b) increased self-reported stress that significantly correlated with decreased IFOF AD in depression. We estimated and confirmed the robustness of differences observed between free-water corrected and uncorrected approaches using bootstrapping. We conclude that applying a free-water correction to DTI data increases the sensitivity of DTI-based metrics to detect clinical effects in MDD.

© 2015 The Authors. Published by Elsevier Inc. This is an open access article under the CC BY-NC-ND license (http://creativecommons.org/licenses/by-nc-nd/4.0/).

1. Introduction

Major depressive disorder (MDD) is a severe and debilitating psychiatric illness, which leads all diseases, psychiatric and otherwise, in terms of lost years of productive life (Organization, 2004). Moreover, conventional pharmacological treatments for depression have shown only modest effectiveness in treating MDD (Trivedi et al., 2006). These modest treatment effects have mandated continued investigation into the biological bases of depression. With the popularization of endocrine assays and structural neuroimaging techniques, depression has been investigated increasingly as a neurodegenerative disorder where stressors leading up to and following the onset of MDD figure prominently in the course of the illness (Sapolsky, 1996, 2000). The formulation of MDD as a neurodegenerative illness has largely born out empirically, with reliable volumetric decreases of limbic and perilimbic regions observed in depression (Campbell et al., 2004;

Goodkind et al., 2015; Hamilton et al., 2008; Videbech and Ravnkilde, 2004). Moreover, data from post-mortem investigations indicate that loss of glial cells is the primary cellular constituent of neurodegeneration in depression (Bowley et al., 2002; Hamidi et al., 2004).

The investigation of neural degeneration in MDD has intensified with the advent of diffusion imaging techniques—such as diffusion tensor imaging (DTI)—for estimating regional white matter microstructure. In understanding depression, the appeal of measuring white-matter structure with techniques such as DTI is twofold. First, DTI could aid in testing hypotheses of MDD as a "disconnection syndrome" in which, for example, activity in limbic regions intensifies due to impaired connectivity with cortical regions implicated in emotional control (Mayberg, 1997; Mayberg et al., 1999). Second, and relatedly, DTI can be used to identify white matter regions that have incurred damage or atrophy potentially due to direct or downstream effects of neurotoxic stress (Lee et al., 2002).

As DTI data in investigations of MDD continue to accrue, there are indications that improvements to this method might be required given that findings have varied considerably across studies. Perhaps the clearest indication of this variability in results is that meta-analyses of DTI findings in MDD have, themselves, yielded disparate findings. For example, two meta-analyses synthesizing reports of regional abnormalities in MDD in fractional anisotropy (FA)—a DTI-based index proposed to reflect axonal organization (Pierpaoli et al., 1996)—yielded findings that were spatially non-overlapping and/or conflicting. One meta-analysis reported FA decreases in the inferior fronto-occipital fasciculus,

inferior longitudinal fasciculus, and posterior thalamic radiation (Liao et al., 2013), while another meta-analysis reported FA decreases in the superior longitudinal fasciculus and FA *increases* in the inferior fronto-occipital fasciculus (Murphy and Frodl, 2011).

The inconsistent findings in DTI investigations of MDD could stem from variability in extra-experimental factors such as gender composition and medication status which, for example, have been shown to account for variability in diffusion imaging studies of schizophrenia (O'Donnell and Pasternak, 2015). It is important to consider, however, that DTI metrics are influenced by contributions of different tissue compartments, including cerebrospinal fluid and extracellular water (Pierpaoli et al., 1996). Thus, if we aim to investigate neural structural pathology in MDD, the partial volume effects of extracellular water that are not part of the tissue could negatively impact the sensitivity and specificity of our DTI metrics. Recently, Pasternak and colleagues developed an algorithm for identifying and separating the effects of extracellular free water on DTI metrics—a process shown to improve DTI-based tract reconstruction (Pasternak et al., 2009) and tissue specificity (Metzler-Baddeley et al., 2012). By using this approach, the effects of extra-cellular free-water on DTI metrics can be removed, leaving them both more sensitive to detecting cellular pathological alterations than standard, uncorrected metrics, and less susceptible to detecting spurious effects aliasing free-water differences. Indeed, this technique has been used to unmask between-group differences in DTI metrics in dementia onset (Maier-Hein et al., 2015), mild cognitive impairment (Berlot et al., 2014), and acute concussion (Pasternak et al., 2014), as well as to identify spurious between-group DTI effects associated with mild cognitive impairment (Berlot et al., 2014), normal aging (Metzler-Baddeley et al., 2012), acute concussion (Pasternak et al., 2014), and schizophrenia (Pasternak et al., 2012b; Pasternak et al., 2015). Finally, free-water correction has been recently applied to one DTI study of MDD, which found a negative correlation between hedonic tone and FA within the medial forebrain bundle (Bracht et al., 2015) in remitted depressed as well as healthy individuals.

In order to systematically assess the usefulness of applying a free-water correction to studies of white-matter integrity in depression, we asked in the present study whether applying a free-water elimination process to DTI data would improve the sensitivity of voxel-wise comparisons of depressed and healthy samples with respect to DTI metrics. These metrics included FA, axial diffusivity (AD), and radial diffusivity (RD). In coherently aligned white matter fibers, AD has been found to be sensitive to identifying axonal degeneration (Wheeler-Kingshott and Cercignani, 2009) and RD has been shown to reliably estimate myelin integrity (Song et al., 2002). We hypothesized that, relative to conventional DTI indices that are not corrected for free water, applying a free-water correction to DTI data would result in improved detection of depression-related abnormalities in DTI metrics, as well as in more statistically reliable correlations between DTI metrics and measures of stress, the latter a process associated with neural degeneration in depression (Sapolsky, 1996).

2. Methods and materials

2.1. Participants

Seventeen females with MDD (38.9 ± 11.4 year; range = 20–55 years) and 18 healthy control (HC) female (33.2 ± 12.0 year; range = 20–55 years) participants were included in this study. Participants were recruited from local psychiatric outpatient clinics as well as through website postings. All participants: (1) were between the ages of 18 and 60; (2) had no reported history of brain injury or lifetime history of primary psychotic ideation or mania; (3) had no reported substance abuse within the past six months; and (4) had no physical limitations that prohibited them from undergoing a magnetic resonance imaging (MRI) examination. No depressed or HC participants were taking psychotropic medication at the time of the study. All depressed participants

met criteria for a DSM-IV diagnosis of MDD on the basis of the Structured Clinical Interview for DSM (SCID; First et al., 1995). None of the control participants met criteria for any current or past DSM Axis I disorder. This study was approved by the Western Institutional Review Board, and all participants signed informed consent prior to study participation.

All participants completed the Beck Depression Inventory-II (BDI-II), and three measures of stress: the Perceived Stress Scale (PSS), the Penn State Worry Questionnaire (PSWQ), and the Panic Disorder Severity Scale (PDSS). The BDI-II is a 21-item self-report instrument that measures depression severity (Beck et al., 1979). The PSS is a 10-item scale developed for measuring the degree to which situations in an individual's life are appraised as stressful (Hewitt et al., 1992). The PSWQ is a 16-item questionnaire for measuring worry at the trait level (Salarifar and Pouretemad, 2012). Finally, the PDSS is a seven-item instrument for measuring severe stressors including acute anxiety and phobia and their consequences with respect to daily functioning (Houck et al., 2002).

2.2. Acquisition of MRI data

Our MRI data were acquired using a 3 Tesla scanner (GE Discovery MR750) with a brain-dedicated receive-only 32-element coil array optimized for parallel imaging (Nova Medical, Inc.). DTI was performed using 30 diffusion-encoding directions (b-value = 1000 s/mm^2, TR/TE = 8800/78.1 ms, with acquisition matrix = 96 × 96, reconstruction matrix = 256 × 256, field of view (FOV) = 25.6 × 25.6 cm, slice thickness = 2 mm, inter-slice spacing 0.2 mm, 69 axial slices, acceleration factor R = 2 in the phase encoding direction) and with one b0 image. T1-weighted anatomical images were acquired using a parallel magnetization-prepared rapid gradient-echo sequence with sensitivity encoding (FOV = 240 mm, 190 slices, slice thickness = 0.9 mm, image matrix = 256 × 256, TR/TE = 5/2.012 ms, acceleration factor R = 2 in the phase encoding direction, flip angle = 8 degrees).

2.3. Preprocessing and analysis

DTI raw data were processed using the Functional Magnetic Resonance Imaging of the Brain (FMRIB) Diffusion Toolbox (FDT; Behrens et al., 2003) included in the FMRIB Software Library (FSL, version 5.0.4; Smith et al., 2004). First, for each participant, a brain mask was defined by applying the Brain Extraction Toolbox (Smith, 2002) to the unweighted image (b-value = 0). Following translation and rotation estimation across acquisitions in three dimensions, the raw DTI images were corrected for motion and eddy currents and relative-motion parameters were estimated from the transformation matrices for each subject (Ling et al., 2012). All individual subject scans with translational or rotational motion estimates greater than three standard deviations (SDs) from the mean were excluded from further analysis. Gradient orientations were compensated prior to calculating b-matrices in order to account for the rotational component of registration. DTI free-water corrected and uncorrected maps were then calculated by using an in-house MATLAB script. The free-water maps were computed by fitting the following model at each voxel (Pasternak et al., 2009):

$$A_g(D, f) = f \exp\left[-bg^T D g\right] + (1-f) \exp\left[-b d_{water}\right]$$

where A_g is the modeled attenuated signal (normalized by b0) for the applied diffusion gradient g, and b is the b-value (1000 s/mm^2). The first term reflects the tissue compartment; D is the diffusion tensor of this compartment, f is the fractional volume of the compartment, and g^T is the transpose of the vector g. The second term reflects an isotropic free-water compartment with a fractional volume of $(1 - f)$; d_{water} is the diffusion coefficient, set to the diffusivity of water at body temperature (3×10^{-3} mm^2/s).

Table 1
Means and standard deviations for age and clinical questionnaire scores.

	MDD (N = 16)	HC (N = 16)	p-value
Mean age ± SD	40.1 ± 10.6	34.8 ± 11.8	>0.10
Mean PSS ± SD	25.0 ± 6.8	11.0 ± 6.6	≪0.05
Mean BDI-II ± SD	27.3 ± 10.8	0.7 ± 1.7	≪0.05
Mean PDSS ± SD	5.13 ± 5.08	0.06 ± 0.25	≪0.05
Mean PSWQ ± SD	60.4 ± 12.0	33.9 ± 7.6	≪0.05

Note: SD = standard deviation; BDI-II = Beck Depression Inventory-II; PSS = Perceived Stress Scale, PDSS = Panic Disorder Severity Scale; PSWQ = Penn State Worry Questionnaire.

To investigate local abnormalities in DTI metrics in white matter in MDD, *with* and *without* free-water correction, we performed a voxel-wise comparison of depressed and HC groups using Tract-Based Spatial Statistics (TBSS) (Smith et al., 2006) on individual maps to which free-water correction procedures were or were not applied. For the TBSS method, the uncorrected FA images (using a threshold of 0.25) were used to generate a group template skeleton and to project the FA values of individual subjects onto that skeleton. Maps for each participant of the additional corrected and uncorrected AD and RD indices, were projected onto the group template skeleton. Within this white-matter skeletonized map, we compared depressed and control groups on a voxel-wise basis with respect to free-water corrected and uncorrected maps of FA, AD, and RD using a family-wise error corrected threshold of $\alpha = .05$. In doing this, we set the number of randomized permutations at 5000 with the threshold-free cluster enhancement option enabled (Smith and Nichols, 2009).

To more rigorously determine the effect of applying free-water elimination, we extracted free-water corrected and uncorrected DTI data from significant clusters identified by our TBSS analysis and subjected these data to additional analysis. In these analyses we tested how free-water elimination affected the magnitude and robustness of group differences, and also whether the elimination improved clinical specificity. To do this, we first computed between-groups effect sizes (Cohen's *d*; Cohen, 1988) from free-water corrected and uncorrected data independently. Then, to determine the reliability of differences in Cohen's *d* statistics resulting from applying versus not applying free-water correction, we used a bootstrapping procedure (Wehrens et al., 2000) in which differences between Cohen's *d* in corrected versus non-corrected data were computed from sampling the data randomly with replacement 10,000 times. Bootstrapping procedures such as this provide an alternative to statistical inference and are used when a parametric model has not or cannot be determined analytically. Bootstrapping can be used to assign accuracy measures—such as confidence intervals—to estimates derived from samples. Non-parametric inferences can then be made regarding these estimates. In the present case, we computed frequency distributions of Cohen's *d* differences and inferred that differences in estimates derived from free-water corrected versus uncorrected data were reliable if the middle 95% of the frequency distribution of Cohen's *d* differences did not intersect with 0.

To understand better the clinical significance of between groups differences in DTI metrics, we computed the Pearson product–moment correlation between DTI metrics and stress measures (PSS, PSWQ, and PDSS) in the depressed group for both free-water corrected and uncorrected DTI data, derived from significant clusters identified by our TBSS analysis (Table 3). Further, to determine the reliability of differences in *r* statistics resulting from applying versus not applying free-water correction, we applied a bootstrapping procedure as presented above to differences in *r* statistics obtained with versus without free-water corrected DTI indices. Importantly, our correlation analyses of the associations between DTI metrics and the different measures of stress were not conceived under the assumption that the stress-related questionnaires render independent information from one another; rather, we used multiple stress measures to determine the robustness of any significant correlations observed with the DTI metrics.

3. Results

Data from two HC participants and one depressed participant were removed from the study due to excessive motion. MDD and HC groups did not differ significantly in age (two-sample *t*-test $p > 0.10$) but, as expected, did differ with respect to BDI-II, PSWQ, PDSS, and PSS scores (all $p \ll 0.05$; please see Table 1).

No significant ($p < 0.05$) differences between groups were found using TBSS analysis of FA, RD, or AD maps, computed *without* free-water correction. In contrast, TBSS analysis on DTI maps *with* free-water correction identified significant decreases in FA and AD (but not RD) in the depressed group relative to the HC group in overlapping clusters within the left inferior fronto-occipital fasciculus (IFOF). [See Fig. 1
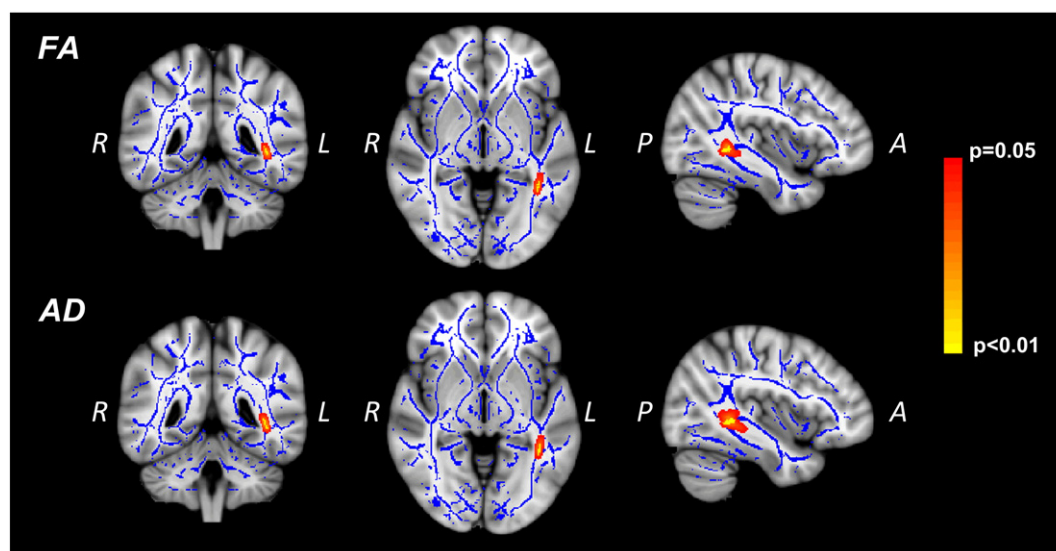

Fig. 1. Clusters where decrements in FA and AD in the MDD relative to the HC group were found when we used the free-water corrected maps. The skeletonized map is shown in blue. The figure is in radiological convention. The MNI coordinates of the centers of mass for AD and FA clusters are (x, y, z): −39, −46, −1 and −39, −43, −1, respectively.
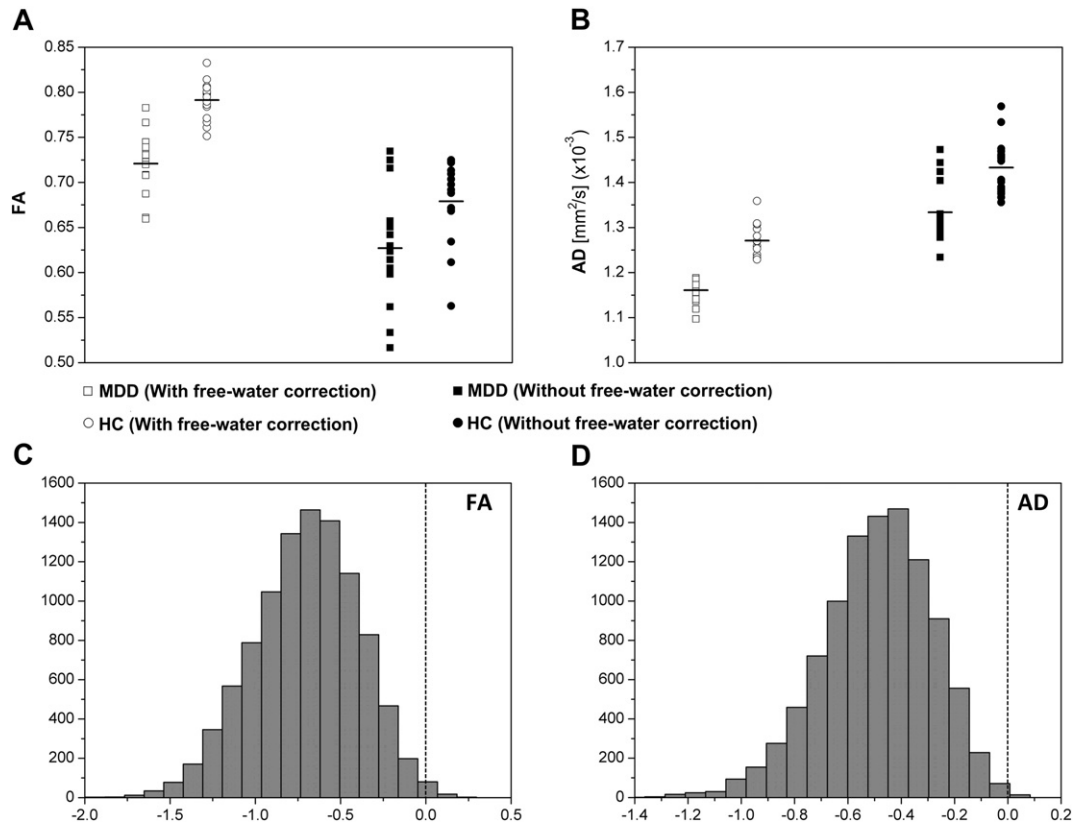
Fig. 2. *Top*: For each group, per-subject FA (A) and AD (B) values from clusters in which a between-groups difference was detected using the free-water correction procedure. For comparison, values derived from uncorrected data are also shown. *Bottom*: For data from these same clusters, bootstrapping-derived distributions of difference in Cohen's *d* obtained *with* versus *without* applying free-water correction prior to estimating FA (C) and AD (D). Dashed lines represent boundaries of middle 95th percentile of distribution of Cohen's *d with* minus *without* free-water correction; that the middle 95th percentile does not intersect with zero indicates the reliability of the difference in Cohen's *d*.

for statistical maps superimposed on the brain and see Fig. 2 (top) for data plots—using both free-water corrected and uncorrected data—from significant FA and AD clusters as obtained from voxel-wise group comparisons of free-water corrected DTI indices.] Of further note, free-water coefficient averages from the clusters in which significant between-groups effects were observed did not differ between the depressed and HC groups (both two-sample *t*-test $p > 0.10$).

Table 2 shows the group means (and standard deviations) and Cohen's *d* values of the between-groups effect size for FA and AD data with and without free-water correction. Our bootstrapping procedure comparing Cohen's *d* for free-water corrected and uncorrected data indicated that the difference observed in the between-groups effects, with corrected versus uncorrected data, are quite robust (see Fig. 2, bottom).

In MDD, we found significant correlations between AD values derived from free-water corrected data and scores from the PSWQ and PDSS (findings for the PSS were marginally significant at $0.05 < p < 0.10$) such that, as scores on these stress measures increased, free-water corrected AD decreased (see Fig. 3 for scatter plots depicting these results). In contrast, we did not observe significant correlations between stress measures and uncorrected AD. Further, the follow-up bootstrap analysis of differences in neural-behavioral correlations with the PSS and PSWQ obtained with corrected versus uncorrected AD data suggest that these differences are robust. We did not observe significant relations between stress measures and either corrected or uncorrected FA.

4. Discussion

In the present study, we investigated whether applying a free-water correction algorithm to DTI data improves the sensitivity to detect

clinical effects in MDD. For free-water corrected, but not for uncorrected data, we found significant reductions in FA and AD (but not RD) in MDD within overlapping clusters in the left IFOF. Moreover, free-water corrected—but not uncorrected—data showed significant correlations with stress measures such that increases in reported stress levels were associated with decreases in free-water-corrected AD in depression. Finally, using a bootstrapping procedure (Wehrens et al., 2000), we noted that differences in the statistics obtained in applying versus not applying the free-water correction were generally quite robust.

While the current study primarily concerns assessing the usefulness of applying free-water correction to diffusion imaging data, the nature and clinical significance of the findings rendered from applying this

Table 2
Means and standard deviations of FA and AD, and Cohen's d-values in MDD and HC groups in the clusters identified by TBSS analysis.

	MDD	HC	Cohen's *d* value
DTI *with* free-water correction Clusters			
FA	0.721 ± 0.033	0.791 ± 0.021	<u>2.531</u>
AD ($\times 10^{-3}$) mm^2/s	1.16 ± 0.03	1.27 ± 0.04	<u>3.111</u>
DTI *without* free-water correction Clusters			
FA	0.627 ± 0.062	0.679 ± 0.044	0.967
AD ($\times 10^{-3}$) mm^2/s	1.33 ± 0.07	1.43 ± 0.06	1.534

Note: FA: fractional anisotropy; AD: axial diffusivity; MDD: major depressive disorder; HC: healthy control. Underlined Cohen's *d* values derived from free-water corrected data show robust differences, as determined by bootstrapping, relative to their non-corrected analogs.

Table 3
Pearson correlation coefficients (r) showing associations between DTI metrics and clinical variables in the MDD group as determined using data with and without free-water correction.

	PSS	PSWQ	PDSS
Free-water corrected map			
FA	r = −0.09	r = 0.14	r = −0.22
AD	r = −0.47*	r = −0.56**	r = −0.62**
Free-water non-corrected map			
FA	r = −0.34	r = 0.23	r = −0.18
AD	r = −0.29	r = 0.15	r = 0.15

Note: FA: fractional anisotropy; AD: axial diffusivity; PSS: Perceived Stress Scale; PSWQ: Penn State Worry Questionnaire; PDSS: Panic Disorder Severity Scale Underlined r values derived from free-water corrected data show robust differences, as determined by bootstrapping, relative to their non-corrected analogs.

* p < 0.07, two-tailed.
** p < .05, two-tailed.

correction bears additional consideration. With respect to discerning the nature of the observed depression-related abnormalities in FA and AD, it is important to consider that while attributing distinct forms of structural pathology to changes in DTI indices has remained challenging (Alexander et al., 2007), two relatively distinct kinds of pathology that can be observed in coherently aligned white matter are demyelination and axonal damage. The relatively high FA values observed in each group, regardless of free-water correction (see Table 2), indicate that we detected a structural abnormality in MDD located in a white-matter region characterized by mostly parallel and well-myelinated fibers (Alexander et al., 2007). The presence of both reduced FA and AD in MDD in overlapping regions of the left IFOF suggests that the decreased anisotropy observed in our MDD sample is most likely due to reduced diffusivity along, as opposed to perpendicular to, this region's

axonal processes. While decreased AD has been found in rodent models of demyelination (Tyszka et al., 2006), increased RD, which was not observed in the present study (indeed, we observed trend-level *decreases* in RD in this region in MDD) has been more reliably associated with demyelination (Song et al., 2005). This leaves open the possibility that reductions in AD in depression are due to axonal damage, a formulation supported by work showing that reduced AD results from cuprizone-induced damage to axons of the corpus callosum in animal models (Sun et al., 2006)—although we hasten to point out here that findings from regions with highly aligned white matter might not extrapolate to regions, like those we identified, with more complex white matter architecture. That we observed reliable correlations in MDD between free-water-corrected AD and measures of stress such that AD decreased as reported stress increased, we propose that stress-related neurodegenerative factors, discussed in detail elsewhere (Sapolsky, 1996), may account for the observed AD reduction in MDD. Nonetheless, other factors such as local glial proliferation or decreased directional coherence of axons in MDD could account for reduced IFOF AD in MDD and correlate to heighted stress in MDD in ways that are not yet well understood.

While other investigations have applied a free-water correction to diffusion imaging data from depressed samples (Bracht et al., 2015), the present study is the first to systematically assess the effect of applying this correction in studies of MDD. In contrast to the findings from Bracht and colleagues, we found significant FA and AD abnormalities in MDD. One explanation for this discrepancy is that the Bracht study focused on MDD in remission whereas we examined current MDD. Our findings taken alongside those from Bracht et al. indicate that FA and AD abnormalities might state- as opposed to trait-related aspects of major depression.

Our current data also begin to address the question of why free-water elimination increases sensitivity to detect effects using diffusion-weighted imaging metrics in MDD. Specifically, we note that we did not find group differences in free-water estimates in those
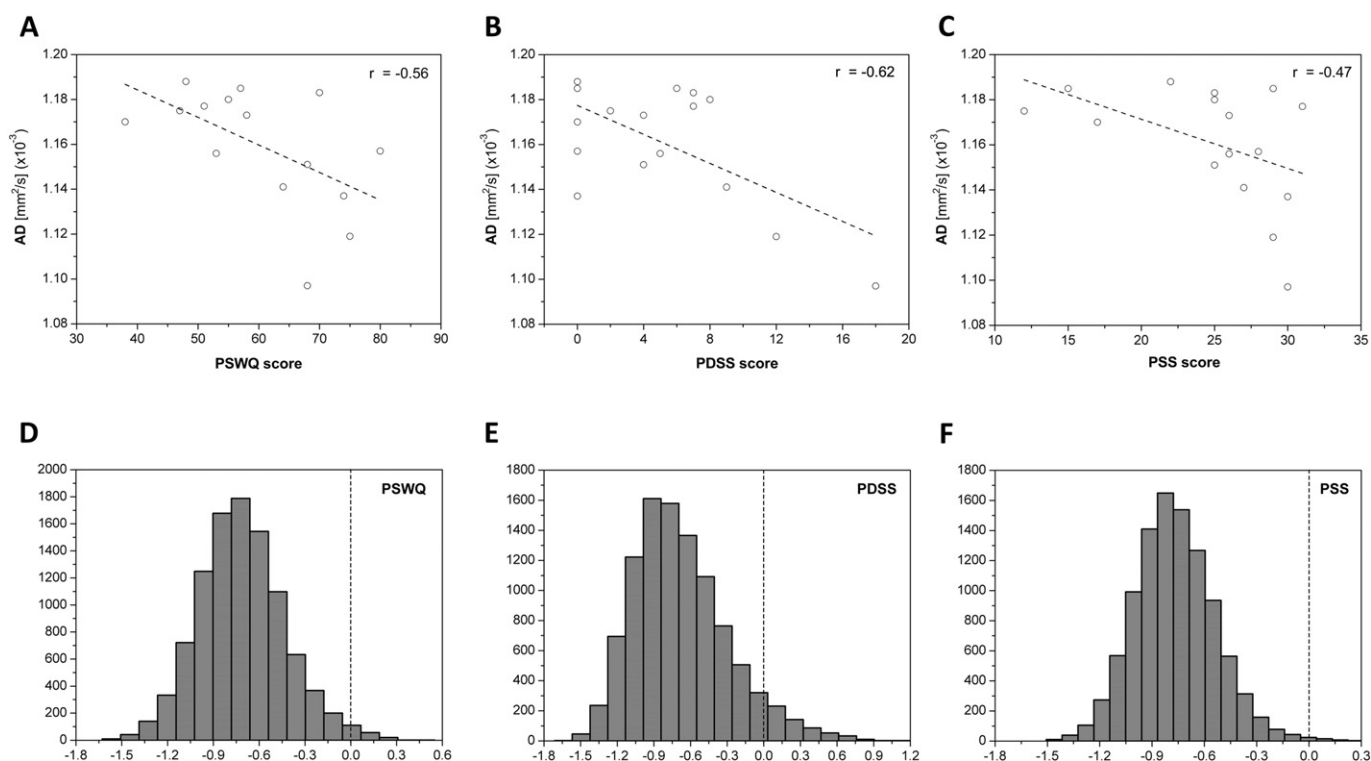

Fig. 3. *Top*: Pearson's correlation between AD values from the cluster in which a between-groups difference was detected using the free-water correction procedure, and (A) PSWQ, (B) PDSS, and (C) PSS scores. *Bottom*: The histograms derived from the bootstrap procedure for assessing the reliability of differences in AD correlations with the PSWQ (D), PDSS (E), and PSS (F) when the free-water correction either was or was not applied. Dashed lines represent boundaries of middle 95th percentile of distribution of r *with* minus *without* free-water correction; that the middle 95th percentile does not intersect with zero in D and F indicates the reliability of the difference in r statistics.

clusters were free-water corrected FA and AD differences were identified. Thus the group differences are likely not attributable to extracellular pathologies such as regional atrophy or neuro-inflammation in MDD. It appears, rather, that decontaminating the diffusion-weighted imaging metrics of free-water effects increased sensitivity by reducing intra-group variability. This can be seen in panels A and B of Fig. 2 where free-water corrected and uncorrected metrics are juxtaposed. Together these results suggest that extracellular partial volume increases intra-group variability, limiting the sensitivity of statistical analyses performed on non-corrected DTI metrics. We note that similar results were found in a dementia onset study (Maier-Hein et al., 2015). Eliminating free-water, therefore, increases the sensitivity to identify group differences, and at the same time increases the specificity to tissue changes, which in MDD increases the clinical specificity to clinical measures.

The current study was based on diffusion MRI data that was acquired with a single b-value shell. This means that the algorithm used to fit the free-water imaging model involved spatial regularization of the data (Pasternak et al., 2009) which decreases intra-group variability, and may obscure subtle spatial features. More advanced acquisitions that include a number of b-value shells enable algorithms that require less dependence on spatial regularization, and may further increase the accuracy of the free-water model (Hoy et al., 2014; Pasternak et al., 2012a), although comparable results using single- and multi-shell acquisitions have been reported (Pasternak et al., 2012a).

There are two important limitations in the present study. First, as we mentioned above, diffusion weighted imaging provides us only with metrics that relate indirectly to neural pathology, and are more ambiguous in areas were fiber bundles are not coherently aligned, leaving the interpretations we make from these metrics in need of additional confirmation from converging methods such as post mortem histological analysis. Second, given that our study samples contained only female participants, our findings might not be generalizable to depression in males.

5. Conclusion

In summary, we present here the first study to determine whether applying a free-water correction algorithm to DTI data improves the sensitivity to detect clinical effects in MDD. We believe this is an important finding as it suggests that such a correction is needed to observe stress-induced neuropathy that is associated with what is likely axonal damage.

Conflict of interest

Dr. Bergamino, Dr. Pasternak, Ms. Farmer, Dr. Shenton, and Dr. Hamilton reported no biomedical financial interests or potential conflicts of interest.

Acknowledgments

References

Alexander, A.L., Lee, J.E., Lazar, M., Field, A.S., 2007. Diffusion tensor imaging of the brain. Neurotherapeutics 4, 316–329.
Beck, A.T., Rush, A.J., Shaw, B.F., Emery, G., 1979. Cognitive Therapy of Depression.
Behrens, T.E., Woolrich, M.W., Jenkinson, M., Johansen-Berg, H., Nunes, R.G., Clare, S., Matthews, P.M., Brady, J.M., Smith, S.M., 2003. Characterization and propagation of uncertainty in diffusion-weighted MR imaging. Magn. Reson. Med. 50, 1077–1088.
Berlot, R., Metzler-Baddeley, C., Jones, D.K., O'Sullivan, M.J., 2014. CSF contamination contributes to apparent microstructural alterations in mild cognitive impairment. NeuroImage 92, 27–35.
Bowley, M.P., Drevets, W.C., Ongur, D., Price, J.L., 2002. Low glial numbers in the amygdala in major depressive disorder. Biol. Psychiatry 52, 404–412.
Bracht, T., Doidge, A.N., Keedwell, P.A., Jones, D.K., 2015. Hedonic tone is associated with left supero-lateral medial forebrain bundle microstructure. Psychol. Med. 45, 865–874.
Campbell, S., Marriott, M., Nahmias, C., MacQueen, G.M., 2004. Lower hippocampal volume in patients suffering from depression: a meta-analysis. Am. J. Psychiatr. 161, 598–607.
Cohen, J., 1988. Statistical Power Analysis for the Behavioral Sciences. second ed. Lawrence Earlbaum Associates, Hillsdale, NJ.
First, M.B., Spitzer, R.L., Gibbon, M., Williams, J.B.W., 1995. The Structured Clinical Interview for DSM-III-R Personality-Disorders (SCID-I). J. Personal. Disord. 9, 83–91.
Goodkind, M., Eickhoff, S.B., Oathes, D.J., Jiang, Y., Chang, A., Jones-Hagata, L.B., Ortega, B.N., Zaiko, Y.V., Roach, E.L., Korgaonkar, M.S., Grieve, S.M., Galatzer-Levy, I., Fox, P.T., Etkin, A., 2015. Identification of a common neurobiological substrate for mental illness. JAMA Psychiatry 72, 305–315.
Hamidi, M., Drevets, W.C., Price, J.L., 2004. Glial reduction in amygdala in major depressive disorder is due to oligodendrocytes. Biol. Psychiatry 55, 563–569.
Hamilton, J.P., Siemer, M., Gotlib, I.H., 2008. Amygdala volume in major depressive disorder: a meta-analysis of magnetic resonance imaging studies. Mol. Psychiatry 13, 993–1000.
Hewitt, P.L., Flett, G.L., Mosher, S.W., 1992. The perceived stress scale — factor structure and relation to depression symptoms in a psychiatric sample. J. Psychopathol. Behav. Assess. 14, 247–257.
Houck, P.R., Spiegel, D.A., Shear, M.K., Rucci, P., 2002. Reliability of the self-report version of the Panic Disorder Severity Scale. Depression and Anxiety 15, 183–185.
Hoy, A.R., Koay, C.G., Kecskemeti, S.R., Alexander, A.L., 2014. Optimization of a free water elimination two-compartment model for diffusion tensor imaging. NeuroImage 103, 323–333.
Lee, A.L., Ogle, W.O., Sapolsky, R.M., 2002. Stress and depression: possible links to neuron death in the hippocampus. Bipolar Disord. 4, 117–128.
Liao, Y., Huang, X., Wu, Q., Yang, C., Kuang, W., Du, M., Lui, S., Yue, Q., Chan, R.C., Kemp, G.J., Gong, Q., 2013. Is depression a disconnection syndrome? Meta-analysis of diffusion tensor imaging studies in patients with MDD. J. Psychiatry Neurosci. 38, 49–56.
Ling, J., Merideth, F., Caprihan, A., Pena, A., Teshiba, T., Mayer, A.R., 2012. Head injury or head motion? Assessment and quantification of motion artifacts in diffusion tensor imaging studies. Hum. Brain Mapp. 33, 50–62.
Maier-Hein, K.H., Westin, C.-F., Shenton, M.E., Weiner, M.W., Raj, A., Thomann, P., Kikinis, R., Stieltjes, B., Pasternak, O., 2015. Widespread white matter degeneration preceding the onset of dementia. Alzheimers Dement. 11, 485–493.
Mayberg, H.S., 1997. Limbic-cortical dysregulation: a proposed model of depression. J. Neuropsychiatr. Clin. Neurosci. 9, 471–481.
Mayberg, H.S., Liotti, M., Brannan, S.K., McGinnis, S., Mahurin, R.K., Jerabek, P.A., Silva, J.A., Tekell, J.L., Martin, C.C., Lancaster, J.L., Fox, P.T., 1999. Reciprocal limbic-cortical function and negative mood: converging PET findings in depression and normal sadness. Am. J. Psychiatr. 156, 675–682.
Metzler-Baddeley, C., O'Sullivan, M.J., Bells, S., Pasternak, O., Jones, D.K., 2012. How and how not to correct for CSF-contamination in diffusion MRI. NeuroImage 59, 1394–1403.
Murphy, M.L., Frodl, T., 2011. Meta-analysis of diffusion tensor imaging studies shows altered fractional anisotropy occurring in distinct brain areas in association with depression. Biol Mood Anxiety Disord 1, 3.
O'Donnell, L.J., Pasternak, O., 2015. Does diffusion MRI tell us anything about the white matter? An overview of methods and pitfalls. Schizophr. Res. 161, 133–141.
Organization, W.H., 2004. The Global Burden of Disease: 2004 Update Geneva.
Pasternak, O., Sochen, N., Gur, Y., Intrator, N., Assaf, Y., 2009. Free water elimination and mapping from diffusion MRI. Magn. Reson. Med. 62, 717–730.
Pasternak, O., Shenton, M.E., Westin, C.-F., 2012a. Estimation of extracellular volume from regularized multi-shell diffusion MRI. Medical image computing and computer-assisted intervention 15, 305–312.
Pasternak, O., Westin, C.-F., Bouix, S., Seidman, L.J., Goldstein, J.M., Woo, T.-U.W., Petryshen, T.L., Mesholam-Gately, R.I., McCarley, R.W., Kikinis, R., Shenton, M.E., Kubicki, M., 2012b. Excessive extracellular volume reveals a neurodegenerative pattern in schizophrenia onset. J. Neurosci. 32, 17365–U17792.
Pasternak, O., Koerte, I., Bouix, S., Fredman, E., Sasaki, T., Mayinger, M., Helmer, K., Johnson, A., Holmes, J., Forwell, L., Skopelja, E., Shenton, M., Echlin, P., 2014. Hockey Concussion Education Project, part 2. Microstructural white matter alterations in acutely concussed ice hockey players: a longitudinal free-water MRI study. J. Neurosurg. 120, 873–881.
Pasternak, O., Westin, C.-F., Dahlben, B., Bouix, S., Kubicki, M., 2015. The extent of diffusion MRI markers of neuroinflammation and white matter deterioration in chronic schizophrenia. Schizophr. Res. 161, 113–118.
Pierpaoli, C., Jezzard, P., Basser, P.J., Barnett, A., Di Chiro, G., 1996. Diffusion tensor MR imaging of the human brain. Radiology 201, 637–648.
Salarifar, M.H., Pouretemad, H., 2012. The study of factor structure, validity and reliability of the Penn State Worry Questionnaire (PSWQ). European Psychiatry 27.
Sapolsky, R.M., 1996. Why stress is bad for your brain. Science 273, 749–750.
Sapolsky, R.M., 2000. Glucocorticoids and hippocampal atrophy in neuropsychiatric disorders. Arch. Gen. Psychiatry 57, 925–935.
Smith, S.M., 2002. Fast robust automated brain extraction. Hum. Brain Mapp. 17, 143–155.
Smith, S.M., Nichols, T.E., 2009. Threshold-free cluster enhancement: addressing problems of smoothing, threshold dependence and localisation in cluster inference. NeuroImage 44, 83–98.
Smith, S.M., Jenkinson, M., Woolrich, M.W., Beckmann, C.F., Behrens, T.E., Johansen-Berg, H., Bannister, P.R., De Luca, M., Drobnjak, I., Flitney, D.E., Niazy, R.K., Saunders, J.,

Vickers, J., Zhang, Y., De Stefano, N., Brady, J.M., Matthews, P.M., 2004. Advances in functional and structural MR image analysis and implementation as FSL. NeuroImage 23 (Suppl. 1), S208–S219.

Smith, S.M., Jenkinson, M., Johansen-Berg, H., Rueckert, D., Nichols, T.E., Mackay, C.E., Watkins, K.E., Ciccarelli, O., Cader, M.Z., Matthews, P.M., Behrens, T.E., 2006. Tract-based spatial statistics: voxelwise analysis of multi-subject diffusion data. NeuroImage 31, 1487–1505.

Song, S.K., Sun, S.W., Ramsbottom, M.J., Chang, C., Russell, J., Cross, A.H., 2002. Dysmyelination revealed through MRI as increased radial (but unchanged axial) diffusion of water. NeuroImage 17, 1429–1436.

Song, S.K., Yoshino, J., Le, T.Q., Lin, S.J., Sun, S.W., Cross, A.H., Armstrong, R.C., 2005. Demyelination increases radial diffusivity in corpus callosum of mouse brain. NeuroImage 26, 132–140.

Sun, S.W., Liang, H.F., Trinkaus, K., Cross, A.H., Armstrong, R.C., Song, S.K., 2006. Noninvasive detection of cuprizone induced axonal damage and demyelination in the mouse corpus callosum. Magn. Reson. Med. 55, 302–308.

Trivedi, M.H., Rush, A.J., Wisniewski, S.R., Nierenberg, A.A., Warden, D., Ritz, L., Norquist, G., Howland, R.H., Lebowitz, B., McGrath, P.J., Shores-Wilson, K., Biggs, M.M., Balasubramani, G.K., Fava, M., Team, S.S., 2006. Evaluation of outcomes with citalopram for depression using measurement-based care in STAR*D: implications for clinical practice. Am. J. Psychiatr. 163, 28–40.

Tyszka, J.M., Readhead, C., Bearer, E.L., Pautler, R.G., Jacobs, R.E., 2006. Statistical diffusion tensor histology reveals regional dysmyelination effects in the shiverer mouse mutant. NeuroImage 29, 1058–1065.

Videbech, P., Ravnkilde, B., 2004. Hippocampal volume and depression: a meta-analysis of MRI studies. Am. J. Psychiatr. 161, 1957–1966.

Wehrens, R., Putter, H., Buydens, L.M.C., 2000. The bootstrap: a tutorial. Chemom. Intell. Lab. Syst. 54, 35–52.

Wheeler-Kingshott, C.A.M., Cercignani, M., 2009. About "axial" and "radial" diffusivities. Magn. Reson. Med. 61, 1255–1260.